16TH EUROPEAN CONFERENCE ON EARTHQUAKE ENGINEERING THESSALONIKI 18 - 21 JUNE 2018

DAMAGE DISTRIBUTION OF THE JUNE 2017 M_w 6.3 LESVOS (NORTH AEGEAN SEA, GREECE) EARTHQUAKE AND EMS-98 APPLICATION TO THE TRADITIONAL SETTLEMENT OF VRISSA

Spyridon MAVROULIS[1], Emmanouil ANDREADAKIS[2], Nafsika-Ioanna SPYROU[3], Varvara ANTONIOU[4], Emmanuel SKOURTSOS[5], Panayotis CARYDIS[6], Efthymios LEKKAS[7]

ABSTRACT

On June 12, 2017, an Mw 6.3 earthquake struck Lesvos (Northeastern Aegean, Greece). Building damage was observed in its southeastern part with very heavy structural damage limited in the traditional settlement of Vrissa. Taking into account that Vrissa is located inland, further from the epicenter than other settlements with less damage, it looks like an earthquake impact paradox. For interpreting this paradox, a rapid field macroseismic reconnaissance was conducted performing not only the classical building-by-building inspection but also use of Unmanned Aircraft Systems (UAS) and Geographic Information Systems (GIS) online applications before any intervention and with the highest possible detail. The dominant structures include old residential buildings with masonry load-bearing walls dated back to the late 19th and early 20th century, reinforced concrete (R/C) buildings and special structures (masonry monumental and industrial buildings). The first category of vulnerability class C constitutes the majority of the building stock and suffered the most with mainly damage grade 5 in the western part of the settlement, special structures also suffered damage grade 4, while the eastern part of Vrissa remained relatively intact. All recent R/C buildings performed well. This difference is attributed mainly to the fact that the most affected northwestern part is founded on Holocene alluvial deposits, while the southeastern intact part on Pleistocene deposits. Moreover, the occurrence of old and highly vulnerable buildings founded on recent deposits in an area characterized by geotechnically unstable zones and bounded by major faults in combination with observed directivity phenomena and possible amplification resulted in destruction in the traditional settlement of Vrissa.

Keywords: building damage; earthquake; Lesvos; EMS-98; masonry buildings

[1]Geologist MSc, PhD Candidate, Department of Dynamic Tectonic Applied Geology, Faculty of Geology and Geoenvironment, School of Sciences, National and Kapodistrian University of Athens, Greece, smavroulis@geol.uoa.gr

[2]Geologist MSc, PhD Candidate, Department of Dynamic Tectonic Applied Geology, Faculty of Geology and Geoenvironment, School of Sciences, National and Kapodistrian University of Athens, Greece, eandreadk@geol.uoa.gr

[3]Geographer MSc, Department of Dynamic Tectonic Applied Geology, Faculty of Geology and Geoenvironment, School of Sciences, National and Kapodistrian University of Athens, Greece, nspyrou@geol.uoa.gr

[4]Geologist PhD, Department of Dynamic Tectonic Applied Geology, Faculty of Geology and Geoenvironment, School of Sciences, National and Kapodistrian University of Athens, Greece, vantoniou@geol.uoa.gr

[5]Geologist PhD, Department of Dynamic Tectonic Applied Geology, Faculty of Geology and Geoenvironment, School of Sciences, National and Kapodistrian University of Athens, Greece, eskourt@geol.uoa.gr

[6]Professor of Earthquake Engineering, Professor Emeritus of the National Technical University of Athens, Greece, Member of the European Academy of Sciences and Arts, Panagouli 5a str., Kifissia, Greece, pkary@tee.gr

[7]Professor of Dynamic Tectonic Applied Geology and Disaster Management, Department of Dynamic Tectonic Applied Geology, Faculty of Geology and Geoenvironment, School of Sciences, National and Kapodistrian University of Athens, Greece, elekkas@geol.uoa.gr

1. INTRODUCTION

On June 12, 2017 (12:28 GMT) a strong earthquake struck Lesvos Island (Northeastern Aegean, Greece) (Fig. 1a). It was estimated to be Mw 6.3 (Papadimitriou et al., 2017). It claimed the life of a woman due to building collapse and 15 injured due to falling debris. Based on preliminary seismological data provided by Papadimitriou et al. (2017), the earthquake epicenter is located offshore southeastern Lesvos (Fig. 1a). The main shock is located at depth of about 13 km and the fault plane solutions demonstrated a NW-SE striking and SW-dipping normal fault that constitutes the northern margin of the offshore Lesvos basin (Fig. 1a).

Building damage induced by the 2017 Lesvos earthquake was localized in southeastern Lesvos. The traditional settlement of Vrissa suffered the most damage to its building stock, while less damage were observed in other villages of the affected area. Almost 50% of buildings that suffered damage by the earthquake are concentrated in Vrissa settlement. More specifically, 472 structures including 408 residential buildings, 25 business premises, 6 temples and public buildings as well as 33 warehouses were characterized as uninhabitable in Vrissa (Natural Disaster Rehabilitation Directorate, 2017).

Taking into account the spatial distribution of damage induced by the 2017 Lesvos earthquake and the fact that Vrissa is located inland, further from the epicenter than other settlements with less damage (e.g. Plomari, Vatera etc) (Fig. 1a), Vrissa seemed like an earthquake impact paradox. Thus, it was decided that an immediate damage assessment should be implemented, with the highest possible detail. In particular, a rapid macroseismic reconnaissance was conducted by the research team throughout the devastated village performing not only classical methods of earthquake damage assessment (e.g. building-by-building inspection), but also modern and innovative techniques, which comprised the use of Unmanned Aircraft Systems (UAS) and Geographic Information Systems (GIS) online applications as the basis of a rapid post-earthquake damage assessment before any intervention was made in the settlement. Thus, all earthquake effects on the natural environment and the building stock of Vrissa were captured and saved with maximum accuracy for further processing and analysis. All data and critical information collected were freely accessible from the link provided (http://arcg.is/2sPnlrf) to all ministries, state authorities, agencies competent in civil protection and disaster management as well as in the direction and coordination of the executive and operational forces at central, regional and local level in order to rapidly and effectively respond to the emergency needs of the affected population arising from the earthquake disaster.

This paper aims to the brief presentation of the geological structure and the recent seismicity of Lesvos and mainly to the application of the European Macroseismic Scale 1998 (EMS-98) based on the guidelines provided by Grünthal (1998) to the area affected by the 2017 Lesvos earthquake with special emphasis to the worst affected settlement of Vrissa by using not only the classical but also modern and innovative methodologies methods of post-earthquake building damage assessment.

2. GEOLOGICAL SETTING AND SEISMICITY OF LESVOS ISLAND

The eastern Lesvos comprises alpine rocks, including a lower unit of Upper Paleozoic to Triassic schists and marbles, underlying tectonically large ultrabasic masses (Lesvos ophiolites) (Hecht, 1972, 1974a, b, c; Katsikatsos et al., 1982; Pe-Piper & Piper, 1993). As regards more recent formations, continental sedimentation occurred during Pleistocene in the coastal region of Vatera located in southeastern Lesvos (Fig. 1a), when a relatively thick sequence of conglomerates and clays was deposited.

The main active tectonic structure of the affected area is the Polichnitos - Plomari fault (Chatzipetros et al., 2013). This NW-SE striking and SW-dipping fault is about 13.5 km (Fig. 1a), controls the long linear series of hills in the areas between Polichnitos and Plomari (Fig. 1a). Its footwall is composed of ophiolites, schists and marbles, while its hanging wall consists of Pleistocene and Holocene deposits (Hecht, 1972, 1974c).

Based on historic and instrumentally recorded seismicity data, it is concluded that the island has been repeatedly struck by earthquakes from 1383 to present with magnitudes varying from 6.2 to 7.4 and seismic intensities of up to X (Papazachos & Papazachou, 2003; Taxeidis 2003; Ambraseys 2009) with significant effects to the local population, the natural environment and the building stock. It is not the first time that the southeastern Lesvos is the worst affected by an earthquake. Similar distribution of seismic intensities were also reported after the 1845 (October 11, M=6.8, I_{MAX}=X), 1867 (March 7, M=7.0, I_{MAX}=X), 1953 (March 18, M=7.4, I_{MAX}=IX+) and 1981 (December 19, M=7.2, I_{MAX}=VIII) (Fig. 1b).

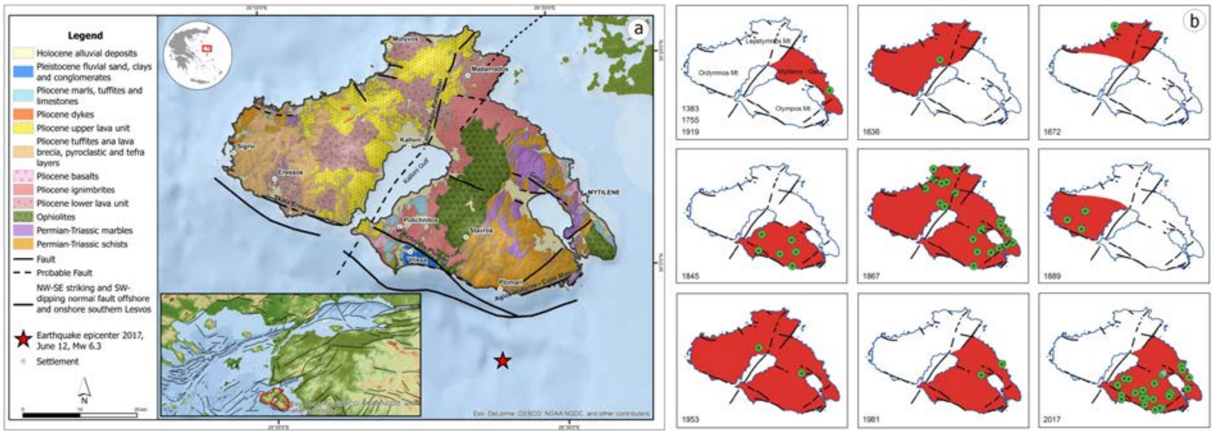

Figure 1. (a) The 2017 Lesvos (Northeastern Aegean Sea, Greece) earthquake was generated offshore southeastern Lesvos by a NW-SE striking and SW-dipping normal fault that constitutes the northern margin of the offshore Lesvos basin located southwards of the island. (b) Areas with high contrasts in seismic intensities during large earthquakes in Lesvos. The maximum intensities have undoubtedly been observed in the southern and eastern part of Lesvos during the 1845, 1867, 1953 and 1981 earthquakes (data from Papazachos & Papazachou, 2003; Taxeidis, 2003; Ambraseys, 2009).

3. APPLICATION OF EMS-98 TO THE TRADITIONAL SETTLEMENT OF VRISSA

3.1. Dominant building types in the affected area and differentiation of buildings into vulnerability classes

During the field phase of the survey more than 1000 buildings were inspected. Generally, the dominant building types of the affected area are: (a) masonry buildings, (b) reinforced-concrete (R/C) buildings, and special structures including (c) monumental and (d) industrial buildings (Fig. 2).
The first category include 1- to 3-storey masonry buildings with load-bearing walls (Fig. 2a-f). These structures can be further classified depending on the construction material of the masonry, which can be composed of (a) massive stones (Fig. 2a-b), (b) manufactured stone units (Fig. 2c-d), (c) mixed materials including massive stones, manufactured stone units, handmade solid clay bricks, perforated bricks and concrete blocks (Fig. 2e-f). These materials are bound by different types of mortar including mainly clay and lime mortars in the old structures and cement mortars in more recent ones. The main characteristic of the masonry buildings is the fact that their construction is dated back to the late 19th and the early 20th century. Consequently, they are at the end of their conventional life cycle and face up probable decay problems affecting the mechanical properties of their elements and their structural response during an earthquake. They belong to the vulnerability class C based on the EMS-98 guidelines. Masonry structures with R/C floors were also observed in the affected area and they also belong to the vulnerability class C.
The second category include R/C buildings with R/C frame comprising horizontal elements (beams) and vertical elements (columns) connected by rigid joints as well as infill-partition walls (Fig. 2g-h). They are recent structures built during the last decades according to strict anti-seismic regulations and specifications and belong to the vulnerability class D. It is significant to note that all new building structures in Lesvos are designed on the basis of a PGA equal to 0.24g, which corresponds to the second largest seismic strength demand according to the Greek seismic code (Earthquake Planning and Protection Organization- EPPO 2000).
During the rapid post-earthquake field survey conducted in Vrissa, a special category of traditional residential buildings was detected. They are characterized by anti-seismic construction with dual structural system. The structures employ both autonomous masonry walls and timber frames with extensive “X” bracing (Fig. 2i). During an earthquake, these frames could guarantee the stability of the

roof in case of a partial collapse of the masonry structure. This system has been also observed in Eressos settlement in the western part of Lesvos and in Bergama in the western coast of Turkey and thoroughly described and analyzed by Karydis (2008).

The third category include masonry monumental structures such as churches and schools (Fig. 2j). Regarding the church construction and architecture in Lesvos, there are few well-preserved and still-standing monuments, mainly of the one-aisled basilica type, representing the church architecture of Lesvos before the 18th century. These structures are characterized of small size, simplicity of the exterior appearance and subtle interior space. Detailed information on building materials, construction methods and architectural design of this period are scarce. This fact is attributed to the high seismicity of the North Aegean region especially during the 19th century and the occurrence of destructive earthquakes from 1845 to 1889, the high vulnerability of these structures due to poor and inadequate construction materials and absence of anti-seismic protection design and measures. The three-aisled basilica was considered to be an innovative type of the church architecture of the early 20th century with many examples observed in Lesvos as well as in Northern Greece. Large three-aisled basilicas were built in sites of older temples. The size and the interior luxury of the churches were indicative of the economic growth and development of this time period. The three-aisled basilica with wooden roof comprises a single stone masonry with a portico and a women chamber above it. The external part of the masonry remained uncovered except from its lower part which was coated in order to give emphasis to the colonnade of the portico. The interior of the basilica along with the colonnade of the aisle and the roof are covered by wooden constructions decorated with secular paintings. Since 19th century, the roof of the central aisle is curved and is decorated with plaster representations and ornaments. The strong tradition of the three-aisled basilica integrated several elements of neoclassicism and western influences towards the end of the 19th century. The high wood-carved temple, often gold-plated and the remarkable post-Byzantine icons uniquely complement the interior of these temples.

Three-aisled basilicas have been built in almost all settlements of Lesvos and are characterized as monuments of Greek traditional architecture. The majority of them are constantly used for cult purposes and unfortunately are systematically altered and face up decay problems attributed to the old construction age and the inappropriate and inadequate preservation methods.

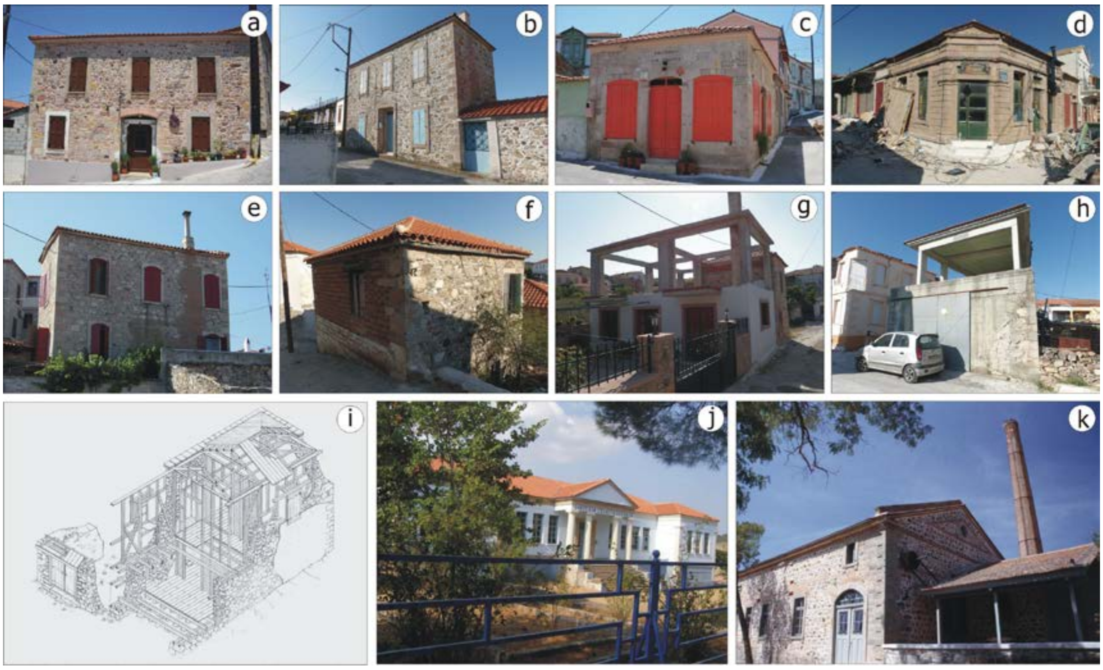

Figure 2: The dominant building types in Vrissa comprise masonry buildings (a-f) and R/C buildings (g-h). The masonry buildings constitutes the majority of the building stock of Vrissa. They mainly include massive stones (a-d) and mixed types including mainly massive stones and perforated bricks (e, f). Their construction is dated back to the late 19th or early 20th century after repeated destructive earthquakes of the 18th century and more specifically from 1845 to 1889. (i) Antiseismic structures with dual structural system were also detected in the affected area. (j-k) Special structures such as school buildings and industrial facilities were also observed.

Many well-preserved buildings of public and private use are of remarkable architecture and serve as reference points for villages of the affected areas. Among these structures, school buildings of great architectural value have been built at the late 19th and the early 20th century even in the most distant and small settlements of Lesvos based on the studies of famous architects of this period. The neoclassical architectural elements include columns supporting the balcony and outer staircase in the entrance. The ground plan of the building is of Π shape and comprises semi-ground and ground spaces located in wings of the buildings used as classrooms, while the central part of the structure includes libraries and the great ceremony hall.
The fourth category include industrial buildings including production structures and their masonry chimneys (Fig. 2k). Lesvos is a geographically isolated area and for this reason its industrial development has started since the 18th century. From the middle 19th century until the liberation in 1921, Lesvos experienced unique moments of economic growth. In 1909, 125 industries were operating in the island including 57 oil presses, 25 soap industries, 17 tanneries, 8 mills, 5 olive-pomace oil factories, spinning mills, dye houses, ginning mills, pasta laboratories, machining centres and talk mines. The construction of new, large and impressive buildings for olive oil extraction and soap production started after 1870 and the arrival of the first steam engines in Lesvos. Nowadays, Lesvos comprises more than 100 well-preserved industrial complexes, whose buildings are defined as architectural monuments. They are still standing, although their static compliance is gradually reduced through the years.

3.2. Damage and its classification into damage grades

The stone masonry buildings suffered the most by the 2017 Lesvos earthquake. They sustained (a) damage grade 1 (negligible to slight damage) comprising hairline cracks in the load-bearing masonry walls, (b) damage grade 2 (moderate damage) including cracks in many walls, detachment of small pieces of places from the walls and partial collapse of chimneys (Fig. 3a), (c) damage grade 3 (substantial to heavy damage) comprising large and extensive cracking of all masonry load-bearing walls, detachment of large pieces of plaster in all load-bearing walls, dislocation and fall of roof tiles, detachment of the roof from the rest of the structure and fall of gables (Fig. 3b), (d) damage grade 4 (very heavy damage) including heavy structural failure of roofs and floors (Fig. 3c) and (e) damage grade 5 of partial and total collapse (Fig. 3d). From the earthquake engineering point of view, the damage observed in this dominant type of structures is attributed mainly to their old construction age and their high vulnerability taking into account the fact that their construction is dated back to the late 19th or the early 20th century.
The special structures including temples, post-byzantine structures, museums, schools and industrial buildings with masonry load-bearing walls suffered similar damage with the masonry residential buildings. More specifically, temples suffered damage comprising cracks in most of the masonry walls (Fig. 3e-f) and in other parts such the dome, the columns, the aisles, the apse and the gable. Post-byzantine structures suffered the aforementioned damage as well as partial collapse of the walls.
Industrial buildings suffered partial collapse of the perimeter masonry walls and damage of the masonry chimneys on the verge of collapse (Fig. 3g-h). A typical example is the industrial building located at the northern entrance of Vrissa settlement comprising an oil mill along with its masonry chimney (Fig. 3g-h). The main building is composed of masonry load-bearing walls built with roughly treated stones and handmade solid clay bricks, while the masonry chimney has been built with solid clay bricks (Fig. 3g-h). Unfortunately, both structures were abandoned since the late 90s, but they were typical examples and reminders of the industrial prosperity of Vrissa during the late 19th century.
Schools suffered fall of the gable above the entrance and partial collapse of the load-bearing masonry walls (Fig. 3i-l).
As regards traditional buildings with the dual structural system, they performed better than the masonry structures with load-bearing walls. The primary structural system comprising the masonry walls of the ground floor sustained no structural damage and light non-structural damage including cracks of the masonry. The secondary structural system showed good performance during the earthquake sustaining successfully the vertical loads of the upper floor and resulting in still standing residential buildings after the earthquake, despite the fact that the masonry suffered damage varying from large cracks to partial collapse.

All R/C buildings constructed during the last decades showed good performance during the 2017 Lesvos earthquake since none of them suffered heavy structural damage. R/C buildings suffered only non-structural damage including cracks in the infill walls, detachment of large pieces of plaster from the infill walls and detachment of the infill walls from the surrounding R/C frame (damage grade varying from 1 to 2 based on the EMS-98). However, some free standing elements sensitive to base accelerations were dislocated and damaged.

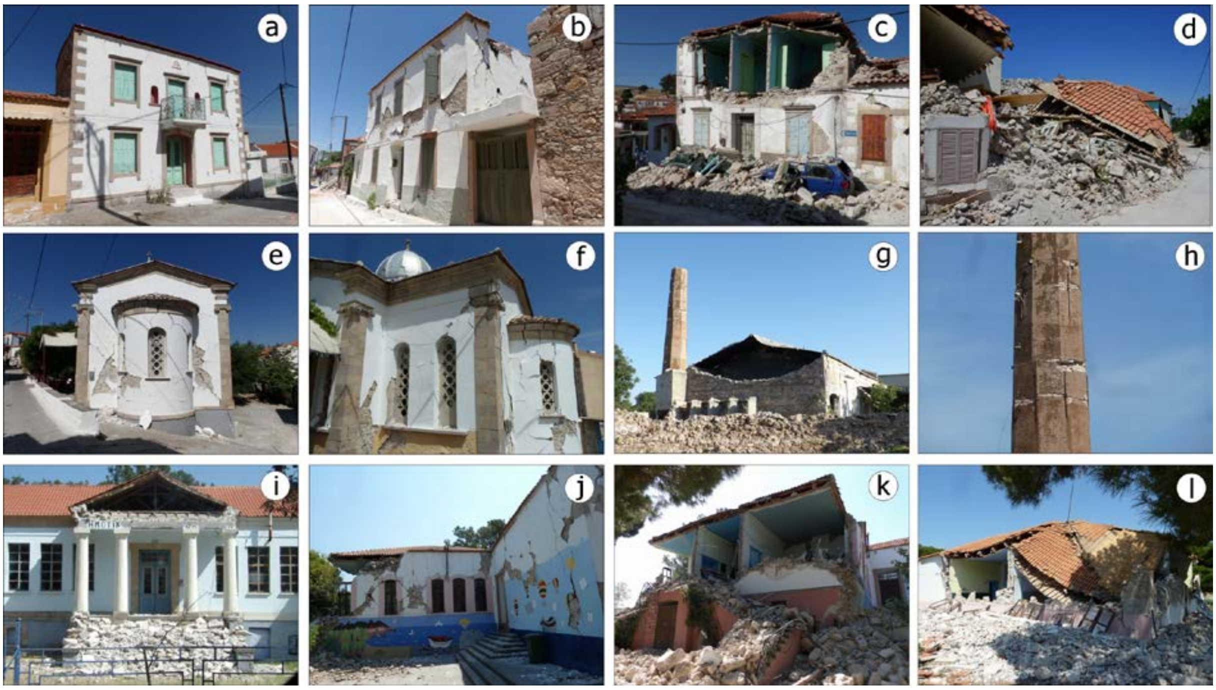

Figure 3. Representative photos of the observed damage in Vrissa settlement. (a) damage grade 2, (b) damage grade 3, (c) damage grade 4 and (d) damage grade 5 in masonry buildings with load-bearing walls. The masonry monumental buildings (e-f) and the masonry industrial builsings and related facilities (g-h) suffered damage similar to masonry residential buildings. (i-l) Masonry schools suffered similar damage. The Vrissa elementary school suffered near total collapse.

Taking into account the aforementioned macroseismic data, among structures constructed without seismic provisions, the stone masonry residential buildings, monumental and industrial structures suffered the most by the earthquake, while the traditional buildings of the area with dual structural system performed relatively well and suffered minor damage. R/C buildings remained intact by the earthquake.

Based on the fact that (a) since 1889 no strong earthquake struck Lesvos until 2017 and (b) Vrissa is a traditional settlement of Lesvos, described as a preserved settlement according to the Governmental Gazette of Hellenic Republic, the majority of buildings include masonry structures belonging to the vulnerability class C (Fig. 4a), while the minority comprises very few R/C buildings belonging to the vulnerability class D (Fig. 4a).

Based on the damage distribution in Vrissa, it is concluded that its northwestern part is the worst affected characterized by damage grades 4 and 5 including partial structural failure of roofs, floors and walls as well as total or near total collapse respectively (Fig. 4b). 47.2% of the surveyed buildings of vulnerability class C suffered damage grade 5, 18.1% damage grade 4, 12.7% damage grade 3, 8.0% damage grade 2 and 13.3% damage grade 1 (Fig. 4b).

3.3. Assignments of EMS-98 intensity degrees and methodology for isoseismal maps drawing

The general idea was to assign local macroseismic intensity values across Vrissa village, taking into account the building damage grades, withdrawing the factor of observation point density and concluding to a clear intensity map.

Almost all buildings (99.38%) in Vrissa belong to vulnerability class C. Consequently, the attempt to determine the macroseismic intensity can only be based on the statistical processing of class C buildings across the different intensity degrees. On the basis of the definitions of quantity (Grünthal, 1998), the minimum and maximum percentages of damaged buildings for each intensity degree were set.

The first attempt was a population density map (Fig. 5a), taking into account the point density of buildings and the damage grade. The map was produced using the centroids of the building polygons to create a Kernel density map, with the number of damage grade used as population value. This map, carries an anisotropy due to not only the damage grade, but also to the shape of the village and the distribution of the surveyed buildings.

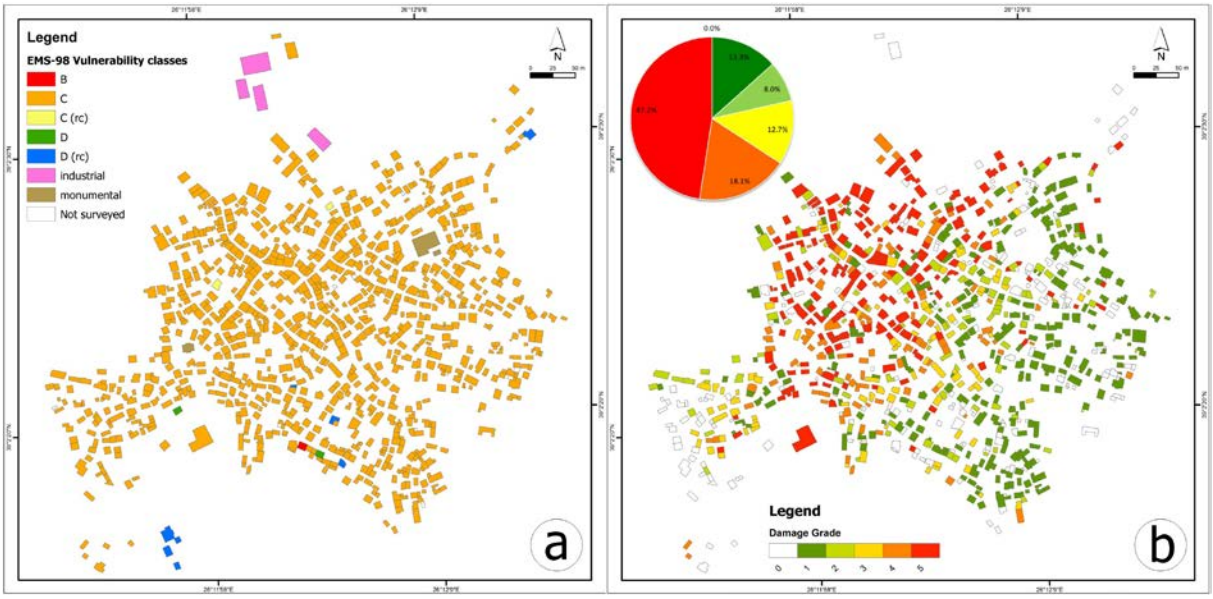

Figure 4. (a) Map of the buildings' vulnerability in Vrissa settlement based on the field macroseismic observations and the EMS-98. A percentage of 99.38% of the buildings are of vulnerability class C. (b) Masonry buildings suffered the most by the 2017 Lesvos earthquake. The observed damage grades varied from 1 to 5 (b). The damage classification into damage grades is based on the EMS-98 (b).

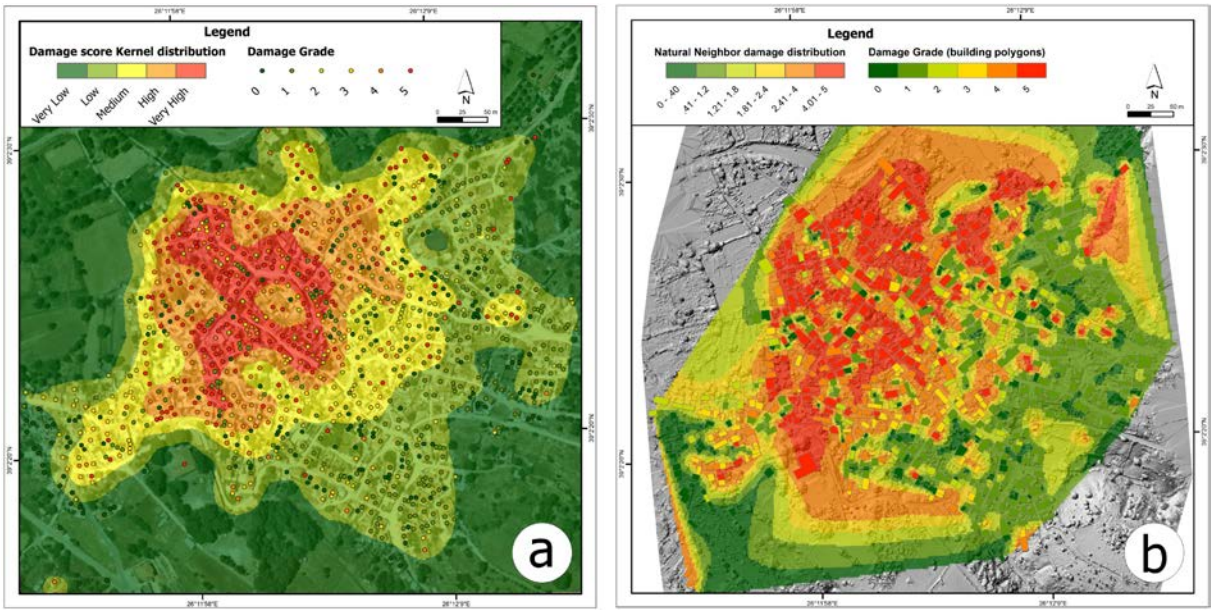

Figure 5: (a) Kernel Damage Score distribution based on point density and damage grade for all buildings (search radius 40m, cell size 1m). (b) Simple interpolation (Natural Neighbor method) of damage grades of vulnerability class C buildings for a search radius circle of 40m. The result respects the recorded values, but it would be more comprehensible if it could be somewhat generalized or smoothened.

This map provides a very good picture of the situation, where the most and worst damage occurred. But it also shows a linear distribution and separation of the village into two sectors, the northwest and the southeast, so provocative that requires further analysis. And before controlling factors are analyzed, there should be a refinement of these results.
The simple interpolation of damage grades for buildings of vulnerability class C was also applied, using the Natural Neighbor for a search radius circle of 40m (Fig. 5b). The result depicts the accurate distribution of damage across the village in accordance with the exact position of buildings, but it would be more comprehensible if it could be somewhat generalized or smoothened.
The purpose of the selected process was to smoothen the resulting map and at the same time withdraw the anisotropy of damage distribution that was due to the shape of the village. Two raster maps were used. The first, was the map of the damage score kernel distribution (Fig. 6a). The second, was the Kernel density of building centroids (with no population=damage grade values), shown in Figure 6b. Dividing the damage score density with the building point density, damage distribution is now weighted and independent from the shape of the village (Fig. 6c). The resulting map is a distribution of a weighted damage grade throughout the area, shown in Figure 6d.
The last step was assigning EMS 98 intensity values to that map. In the following Table 1, the calculations of Damage Score (=point density in Number of Houses * Damage Grade per house per square kilometer, N*D/km^2) as a function of building density is shown. Then, the minimum and maximum scores are selected and divided with the given point density, to provide an index that represents a minimum and maximum Weighted Damage Grade, which is characteristic of the damage grade of the Vulnerability Class for every intensity degree (Fig. 6e).

Table 1: Minimum and Maximum Damage Score as a function of building point density, and Weighted Damage Grade, independent of Building Point Density, for each Intensity Degree (VII-XII, descending).

C-Vulnerability class

Damage Grade	House Centroid Density (N/km^2)	Damage points (Grade*N/km^2)	Minimum Percentage for XII_{EMS-98}	Maximum Percentage for XII_{EMS-98}	Minimum Damage Score for XII_{EMS-98}	Maximum Damage Score for XII_{EMS-98}	Minimum Weighted Damage (Minimum Damage Score/House Density) for XII_{EMS-98}	Maximum Weighted Damage (Minimum Damage Score/House Density) for XII_{EMS-98}
0	1000	0					4	5
1	1000	1000						
2	1000	2000						
3	1000	3000						
4	1000	4000						
5	1000	5000	80%	100%	4000	5000		
Damage Grade	House Centroid Density (N/km2)	Damage points (Grade*N/km2)	Minimum Percentage for XI_{EMS-98}	Maximum Percentage for XI_{EMS-98}	Minimum Damage Score for XII_{EMS-98}	Maximum Damage Score for XII_{EMS-98}	Minimum Weighted Damage (Minimum Damage Score/House Density) for XI_{EMS-98}	Maximum Weighted Damage (Minimum Damage Score/House Density) for XI_{EMS-98}
0	1000	0					1	4
1	1000	1000						
2	1000	2000						
3	1000	3000						
4	1000	4000	60%	100%	2400	4000		
5	1000	5000	20%	60%	1000	3000		
Damage Grade	House Centroid Density (N/km^2)	Damage points (Grade*N/km^2)	Minimum Percentage for X_{EMS-98}	Maximum Percentage for X_{EMS-98}	Minimum Damage Score for X_{EMS-98}	Maximum Damage Score for X_{EMS-98}	Minimum Weighted Damage (Minimum Damage Score/House Density) for X_{EMS-98}	Maximum Weighted Damage (Minimum Damage Score/House Density) for X_{EMS-98}
0	1000	0					0	2.4
1	1000	1000						

2	1000	2000						
3	1000	3000						
4	1000	4000	20%	60%	800	2400		
5	1000	5000	0%	20%	0	1000		

Damage Grade	House Centroid Density (N/km^2)	Damage points (Grade*N/km^2)	Minimum Percentage for IX$_{EMS-98}$	Maximum Percentage for IX$_{EMS-98}$	Minimum Damage Score for IX$_{EMS-98}$	Maximum Damage Score for IX$_{EMS-98}$	Minimum Weighted Damage (Minimum Damage Score/House Density) for IX$_{EMS-98}$	Maximum Weighted Damage (Minimum Damage Score/House Density) for IX$_{EMS-98}$
0	1000	0					0	1.8
1	1000	1000						
2	1000	2000						
3	1000	3000	20%	60%	600	1800		
4	1000	4000	0%	20%	0	800		
5	1000	5000						

Damage Grade	House Centroid Density (N/km^2)	Damage points (Grade*N/km^2)	Minimum Percentage for VIII$_{EMS98}$	Maximum Percentage for VIII$_{EMS98}$	Minimum Damage Score for VIII$_{EMS-98}$	Maximum Damage Score for VIII$_{EMS-98}$	Minimum Weighted Damage (Minimum Damage Score/House Density) for VIII$_{EMS98}$	Maximum Weighted Damage (Minimum Damage Score/House Density) for VIII$_{EMS-98}$
0	1000	0					0	1.2
1	1000	1000						
2	1000	2000	20%	60%	400	1200		
3	1000	3000	0%	20%	0	600		
4	1000	4000						
5	1000	5000						

Damage Grade	House Centroid Density (N/km^2)	Damage points (Grade*N/km^2)	Minimum Percentage for VII$_{EMS-98}$	Maximum Percentage for VII$_{EMS-98}$	Minimum Damage Score for VII$_{EMS-98}$	Maximum Damage Score for VII$_{EMS-98}$	Minimum Weighted Damage (Minimum Damage Score/House Density) for VII$_{EMS-98}$	Maximum Weighted Damage (Minimum Damage Score/House Density) for VII$_{EMS-98}$
0	1000	0					0	0.4
1	1000	1000						
2	1000	2000	0%	20%	0	400		
3	1000	3000						
4	1000	4000						
5	1000	5000						

Finally, intensity degrees were matched to weighted damage grades according to the boundaries of Figure 6e, and the weighted damage grade map for vulnerability class C buildings, was translated into EMS 98 intensity map, as shown in Figure 6f.

Different algorithms and parameters were used in order to optimize the resulting intensity map. Simple Point Density results in a more fragmented map, while Kernel Density provides a smoother and more generalized map and contours. Also, different search radius values were tested. This parameter depends on the area extent and number of observation points. Automatic settings (in this case 16m, 1/30th of the minimum dimension of the map) resulted in a bubble-like map (circular areas around the house centroids), while a larger radius (50m) resulted in losing one intensity degree due to over-generalization. Through a trial and error process, a search radius of 40 meters was finally selected as the most suitable for conditions at hand. The processing steps are shown in Figure 6.

We conclude that this Weighted Damage Grade Map is equivalent to an EMS-98 Macroseismic Intensity Map (Fig. 6f). It has to be noted that, on the basis of C Class vulnerability buildings, damage statistics would justify an intensity of XII, once there are areas that all such constructions have collapsed. However, it was decided to mark these areas with an XI+, because there were not enough R/C buildings in the area, and assigning a XII intensity would be reasonably questionable.

4. CONCLUSIONS – DISCUSSION

Based on the results of the field reconnaissance in the devastated settlement of Vrissa, it is concluded that residential buildings with masonry load-bearing walls dated back to the late 19th and early 20th century comprise the majority of the building stock. Mainly due to their old construction age and their high vulnerability, they suffered the most by the 2017 Lesvos earthquake. Based on the EMS-98, they classified mainly into vulnerability class C and they suffered mostly damage grade 5 and 4 (47.2% and 18.1% of the total buildings of Vrissa respectively). Special structures including temples, post-byzantine structures, museums, schools and industrial buildings with masonry load-bearing walls suffered similar damage with the masonry residential buildings. All R/C buildings constructed during the last decades showed good performance during the 2017 Lesvos earthquake since none of them suffered heavy structural damage.

During the rapid post-earthquake field survey conducted in the affected area, a special category of traditional residential buildings was detected in Vrissa settlement. These traditional buildings are characterized by dual structural system comprising both autonomous masonry walls and timber frames with extensive “X” bracing. These frames guaranteed the stability of the roof and the structures did not collapse even in the case of partial collapse of their masonry walls.

In conclusion, an $XI+_{EMS\text{-}98}$ intensity was mainly assigned to the western part of Vrissa settlement and in isolated areas of its southern part due to the fact that most buildings of vulnerability class C suffer damage of grade 4 and many of grade 5. Taking into account the methodology applied for the EMS-98 seismic intensities assignment in Vrissa settlement, the following remarks can be made:

i. Damage assessment was only applicable for C Class buildings, due to their overwhelming majority in the settlement (>99%).
ii. Most of buildings with damage grade 5 were located within the area of low slope angles and low elevation, with the exception of the southwestern part of the village.
iii. Raw damage distribution shows a linear development of maximum damage for the northwest part of the village. However, this shape is biased by the building distribution and density of the village.
iv. Weighted damage distribution shows a NNE-SSW zone of maximum damage, equivalent to $XI+_{EMS\text{-}98}$ intensity.

The very heavy structural damage was observed in the western part of Vrissa, while its eastern part remained relatively intact (Fig. 6f-g). Taking into account the geological and tectonic structure, the geomorphological setting and our field macroseismic observations on the type, vulnerability and damage grades of buildings, it is concluded that the worst affected part of Vrissa is founded on Holocene alluvial deposits comprising gray and red clays, sands and gravels, while the slightly affected part is founded on Pleistocene deposits including fluvial sands, clays and conglomerates with thickness of about 100 m (Fig. 6h).

Apart from the worst affected western part of Vrissa founded on alluvial deposits, very heavy structural damage including partial or total collapses was also observed in isolated areas in its southwestern intact part. The occurrence of these damage islet is attributed to the generation of earthquake-induced landslides along geotechnically unstable zones characterized by relatively steeper slopes (Fig. 6g).

Based on data and results of this field macroseismic survey after the June 12, 2017 Lesvos earthquake, it is concluded that the geological setting, the geomorphological parameters, the occurrence of geotechnically unstable zones, the geotechnical properties of the foundation soils and the building characteristics in the devastated village have been identified as factors controlling the spatial distribution of building damage in Vrissa settlement. More specifically, the occurrence of buildings characterized by old construction age and high vulnerability founded on recent deposits and on slopes in an area that it is bounded by significant faults in combination with observed directivity phenomena detected by Papadopoulos et al. (2017) and possible amplification resulted in destruction.

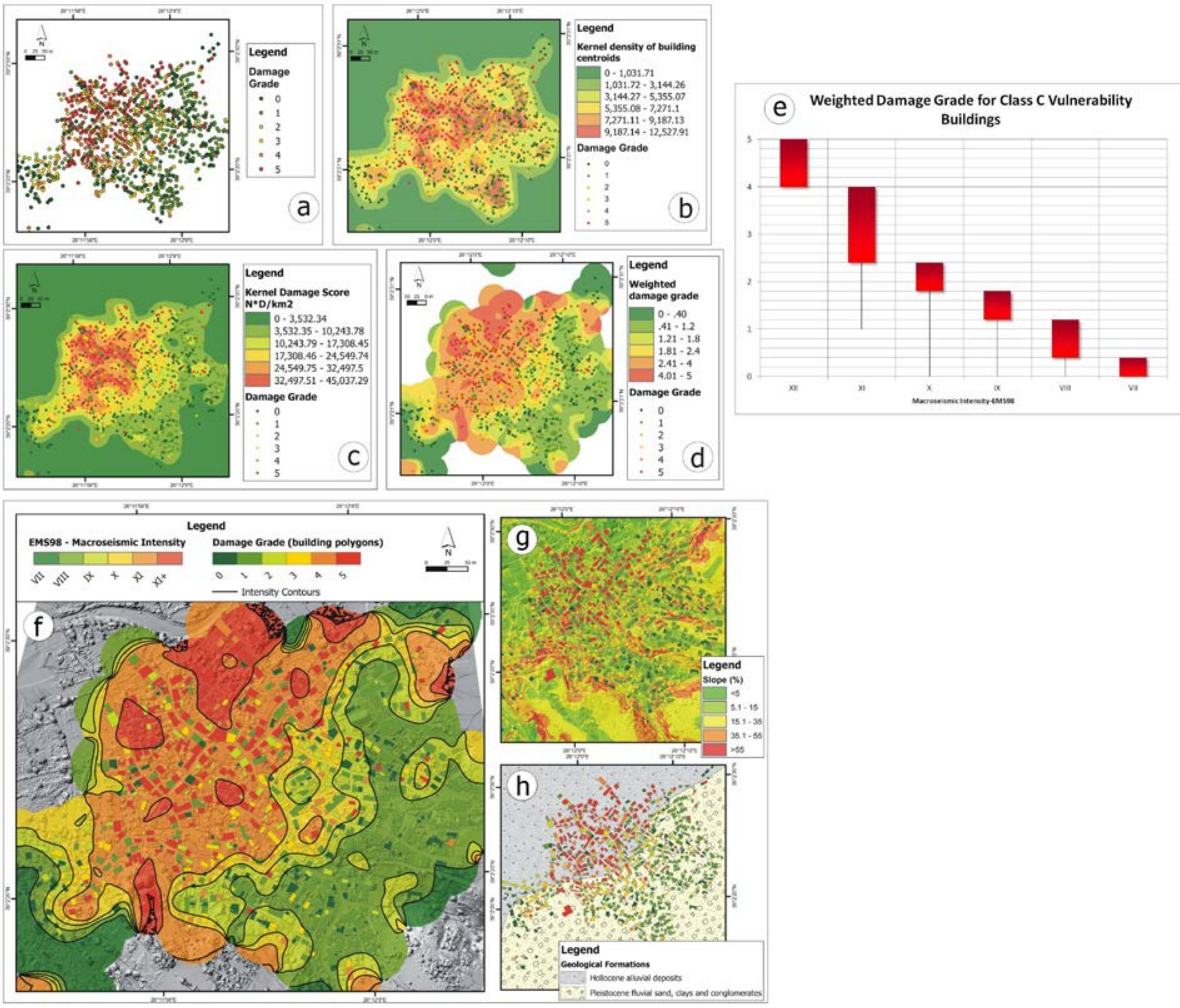

Figure 6. (a) Building polygons converted to points (feature to point) for further point density calculations. (b) Kernel density of building centroids. (c) Kernel Damage Score map (Damage Grade*Point Density/km^2). (d) Weighted Damage Grade (Kernel Damage Score Map/Kernel Point Density Map). (e) Weighted Damage Grade and respective EMS-98 Intensity degrees. (f) Isoseismal map for Vrissa settlement after the 2017 Lesvos earthquake based on the application of the EMS-98. (g) Geological map of the broader area of Vrissa. (h) Slope map of Vrissa (values %).

5. REFERENCES

Ambraseys N (2009). Earthquakes in the Mediterranean and Middle East: a multidisciplinary study of seismicity up to 1900. Cambridge University Press.

Chatzipetros A, Kiratzi A, Sboras S, Zouros N, Pavlides S (2013). Active faulting in the north-eastern Aegean Sea Islands. *Tectonophysics*, 597-598: 106-122.

Earthquake Planning and Protection Organization (2000). Greek Antiseismic Code 2000- EAK 2000, Athens: Ministry of Environment, Planning and Public Works.

Grünthal G. (ed) (1998). European Macroseismic Scale 1998 EMS-98, Conseil de l’Europe, Cahiers du Centre Européen de Géodynamique et de Séismologie, 15, Luxembourg.

Hecht J (1972). Geological map of Greece, Plomari-Mytilini sheet. Institute of Geology and Mineral Exploration of Greece scale 1:50.000.

Hecht J (1974a). Geological Map of Greece, Methymna sheet. Institute of Geology and Mineral Exploration of Greece scale 1:50.000.

Hecht J (1974b). Geological map of Greece, Eressos sheet. Institute of Geology and Mineral Exploration of Greece scale 1:50.000.

Hecht J (1974c). Geological map of Greece, Polichnitos sheet. Institute of Geology and Mineral Exploration of Greece scale 1:50.000.

Karydis N (2008) Traditional antiseismic structure in the Eastern Aegean: The case of Eressos and Pergamon, *Proceedings of the 3rd Panhellenic Conference on Earthquake Engineering & Seismology*, 5-7 November 2008, Athens, Greece.

Katsikatsos G, Mataragas D, Migiros G, Triandafillou E (1982). Geological study of Lesbos Island, Special Report, IGME.

Natural Disaster Rehabilitation Directorate (2017) Results from the first building inspection after 2017 Lesvos earthquake from June 13th to June 24th 2017.

Papadimitriou P, Tselentis G-A, Voulgaris N, Kouskouna V, Lagios E, Kassaras I, Kaviris G, Pavlou K, Sakkas V, Moumoulidou A, Karakonstantis A, Kapetanidis V, Sakkas G, Kazantzidou D, Aspiotis T, Fountoulakis I, Millas C, Spingos I, Lekkas E, Antoniou V, Mavroulis S, Skourtsos E, Andreadakis E (2017). Preliminary report on the Lesvos 12 June 2017 Mw=6.3 earthquake. Euro-Med Seismological Centre (EMSC).

Papazachos BC, Papazachou CB (2003). The earthquakes of Greece. Ziti Publ., Thessaloniki, Greece, p 286.

Pe-Piper G, Piper DJW (1993). Revised stratigraphy of the Miocene volcanic rocks of Lesvos, Greece. *Neues Jahrbuch Geologie und Palaeontologie Munchen*, 2: 97-110.

Taxeidis K (2003). Study of Historical Seismicity of the Eastern Aegean Islands. PhD thesis, National and Kapodistrian University of Athens, Greece, 301 pp. http://macroseismology.geol.uoa.gr/studies/TAXE003.pdf